lytical Methods Inc., Washington, DC, 1982.

[7]Lan, C. E., and S. C. Mehrotra, "An Improved Woodward's Panel Method for Calculating Leading-Edge and Side-Edge Suction Forces at Subsonic and Supersonic Speeds," NASA CR 3205, 1979.

[8]Hardy, B. C., and S. P. Fiddes, "Prediction of Vortex Lift on Non-Planar Wings by the Leading-Edge Suction Analogy," *Aeronautical Journal*, Vol. 92, No. 914, 1988, 154–164.

Wing Mass Formula for Subsonic Aircraft

Sergei V. Udin* and William J. Anderson†
University of Michigan, Ann Arbor, Michigan 48109

Description

MOST wing mass formulae[1,2] are based on statistical information. As a consequence, these formulae usually have good accuracy only on a restricted set of wing data. A theoretical wing mass derivation based on a simplified concept model of a wing is presented in Ref. 3. This method takes into consideration all the details of the aircraft wing, including complicated geometry and concentrated loads, such as the engines. Formulae to estimate mass due to swept moment, mass due to twist moment, and mass due to shear are presented below. The mass of other wing components, which total about 30% of the wing mass, can be estimated by known methods.[1,4] The reader is referred to a complete and detailed derivation in Ref. 5.

The geometry of a subsonic aircraft wing with span b is shown in Fig. 1. We define the *inboard wing* as the part of the wing between the fuselage joints. It is assumed that the inboard wing section is not tapered and not swept. The *midboard wing* is the part of the wing between the fuselage joint and the sweep joint. The *outboard wing* lies between the sweep joint and the wing tip. We consider that the aircraft has no inboard wing concentrated loads, has n_m i-numbered midboard wing concentrated loads, and has n_o j-numbered outboard wing concentrated loads. The relative mass of each load is $\frac{1}{2}m_c^i$ or $\frac{1}{2}m_c^j$ (i.e., m_c^i or m_c^j is the mass of both symmetric loads located in both parts of the wing). The relative coordinate of a concentrated load (absolute Z^i or Z^j coordinate divided by half-span) is z_c^i or z_c^j.

The estimated relative mass of the wing structure is

$$m_w = k_{tm}(m_M + m_Q) + m_{\text{rib}} + m_{\text{ail}} + m_{\text{sk}} + m_{\text{flap}} \tag{1}$$

The formulae to estimate relative masses of ribs m_{rib}, ailerons m_{ail}, load-free skin m_{sk}, and flaps m_{flap} are presented in Refs. 1, 2, and 4. The twist moment factor k_{tm} is

$$k_{tm} = 1 + \frac{0.015\sqrt{A}(1 + 2\lambda_t)}{(1 + \lambda_t)\cos\Lambda} \tag{2}$$

where A is the aspect ratio, λ_t is the taper ratio to wing tip (wing tip chord divided by wing root chord), and Λ is the half-chord wing sweep.

Received May 6, 1991; accepted for publication May 28, 1991.

*Visiting Research Scholar, Aerospace Engineering Department. Permanent affiliation: Graduate Student, Moscow Aviation Institute, Moscow, Russia.

†Professor of Aerospace Engineering. Senior Member AIAA.

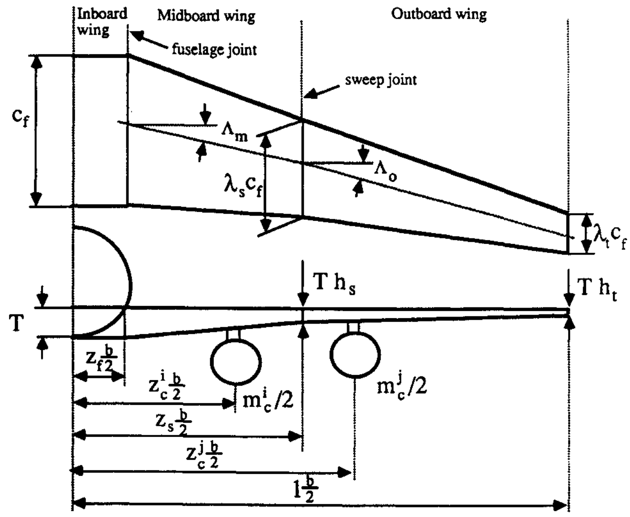

Fig. 1 Wing geometry.

The relative masses of structure counteracting the bending moment and shear are

$$m_M = \left(\frac{\rho_{\text{lower}}}{\sigma_{\text{act lower}}} + \frac{\rho_{\text{upper}}}{\sigma_{\text{act upper}}}\right)\frac{Ag_d a\mu E_T}{4pT}(K_{M_i} + K_{M_m} + K_{M_o}); \quad m_Q = 0.1\, m_M \tag{3}$$

where ρ_{lower} and ρ_{upper} are densities of lower and upper panel structural materials, g_d is the design overload factor, a is gravitational acceleration, μ is the mass of the aircraft, and p is wing loading. The approximate value of effective airfoil thickness coefficient E_T is

$$E_T \approx 1.1\left(\frac{4T_2}{T_1 + 2T_2 + T_3}\right)^2 \approx 1.2 \cdot\cdot 1.4 \tag{4}$$

where T_1 is the first spar height, T_2 is the maximum airfoil height, and T_3 is the most rearward spar height. The values of actual stresses averaged over the lower panel volume $\sigma_{\text{act lower}}$ and the values of actual stresses averaged over the upper panel volume $\sigma_{\text{act upper}}$ can be obtained from the statistics of an aircraft with approximately the same mass, size, and manufacturing quality. These values also can be estimated as

$$\sigma_{\text{act lower}} = \frac{\sigma_{u\,\text{lower}}}{k_{sl\,\text{lower}}k_{\text{man}}}; \qquad \sigma_{\text{act upper}} = \frac{\sigma_{u\,\text{upper}}}{k_{sl\,\text{upper}}k_{\text{man}}}, \tag{5}$$

where the coefficient $k_{sl\,\text{lower}}$ is the lower panel ultimate stress $\sigma_{u\,\text{lower}}$ divided by the permissible fatigue lower panel stress, $k_{sl\,\text{upper}}$ is upper panel ultimate stress $\sigma_{u\,\text{upper}}$ divided by the permissible fatique upper panel stress and the manufacturing coefficient k_{man} has expert value within bounds presented in Table 1. The value of k_{man} decreases when the dimensions and mass of aircraft are increased. If the absolute root wing thickness T does not exist, it can be inferred from the overall geometry as

$$T = \frac{2t_r}{(\lambda_t + \lambda_s)(1 - z_s) + (1 + \lambda_s)(z_s - z_f) + 2z_f}\sqrt{\frac{\mu}{pA}} \tag{6}$$

where t_r is the root relative thickness; λ_s is the taper ratio to the sweep joint (chord at sweep joint divided by root chord); z_s is the relative coordinate of sweep joint; and z_f is the relative coordinate of fuselage joint. The coefficients K_{M_o}, K_{M_m}, and K_{M_i} in Eq. (3) are

$$
\begin{aligned}
K_{M_o} = {} & \frac{1-z_s}{(h_s-h_t)\cos\Lambda_o}\left\{\frac{(1-z_s)^2}{3(h_s-h_t)^3}\left(h_t^3\left(\ln\left(\frac{h_t}{h_s}\right)-\frac{11}{6}\right)+\frac{h_s^3}{3}-\frac{3}{2}h_t h_s^2+3h_t^2 h_s\right)\right. \\
& \times\left(\frac{1-\lambda_t}{z_s(1-\lambda_t)+\lambda_t+1}-\frac{(\psi_s-\psi_t)m_{fu}}{(1+\psi_s)(z_s-z_f)+(\psi_s+\psi_t)(1-z_s)}-\frac{m_w^*}{9z_f+6(z_s-z_f)+2(1-z_s)}\right) \\
& +\left(\frac{1-z_s}{h_s-h_t}\right)^2\left(h_t^2\left(\ln\left(\frac{h_s}{h_t}\right)+\frac{3}{2}\right)+\frac{h_s^2}{2}-2h_t h_s\right) \\
& \times\left(\frac{\lambda_t}{z_s(1-\lambda_t)+\lambda_t+1}-\frac{\psi_t m_{fu}}{(1+\psi_s)(z_s-z_f)+(\psi_s+\psi_t)(1-z_s)}-\frac{\frac{1}{2}m_w^*}{9z_f+6(z_s-z_f)+2(1-z_s)}\right) \\
& \left.-\sum_{j=1}^{no} m_c^j\left[z_c^j-z_s+\left(h_t\frac{1-z_s}{h_s-h_t}+1-z_c^j\right)\ln\left(\frac{\frac{1-z_c^j}{1-z_s}(h_s-h_t)+h_t}{h_s}\right)\right]\right\}; \\
K_{M_m} = {} & \frac{z_s-z_f}{(1-h_s)\cos\Lambda_m}\left\{\frac{(z_s-z_f)^2}{(1-h_s)^3}\left(\frac{1}{3}-\frac{3}{2}h_s+3h_s^2-\frac{11}{6}h_s^3+h_s^3\ln(h_s)\right)\right. \\
& \times\left(\frac{-m_w^*}{9z_f+6(z_s-z_f)+2(1-z_s)}+\frac{-\frac{1}{3}(1-\psi_s)m_{fu}}{(1+\psi_s)(z_s-z_f)+(\psi_s+\psi_t)(1-z_s)}\right) \\
& +\left(\frac{z_s-z_f}{1-h_s}\right)^2\left(\frac{1}{2}-2h_s+\frac{3}{2}h_s^2-h_s^2\ln(h_s)\right) \\
& \times\left(\frac{1}{z_s(1-\lambda_t)+\lambda_t+1}-\frac{\psi_s m_{fu}}{(1+\psi_s)(z_s-z_f)+(\psi_s+\psi_t)(1-z_s)}-\frac{\frac{3}{2}m_w^*}{9z_f+6(z_s-z_f)+2(1-z_s)}\right) \\
& +\left(\frac{z_s-z_f}{1-h_s}\right)(1+h_s\ln(h_s)-h_s)\left(\frac{(1-z_s)(1-\lambda_t)}{z_s(1-\lambda_t)+\lambda_t+1}\right. \\
& \left.-\frac{(1-z_s)(\psi_s+\psi_t)m_{fu}}{(1+\psi_s)(z_s-z_f)+(\psi_s+\psi_t)(1-z_s)}-\frac{2(1-z_s)m_w^*}{9z_f+6(z_s-z_f)+2(1-z_s)}\right) \\
& -\ln(h_s)\left(\frac{(1-z_s)^2\left(\frac{1}{3}+\frac{2}{3}\lambda_t\right)}{z_s(1-\lambda_t)+\lambda_t+1}-\frac{(1-z_s)^2\left(\frac{1}{3}\psi_s+\frac{2}{3}\psi_t\right)m_{fu}}{(1+\psi_s)(z_s-z_f)+(\psi_s+\psi_t)(1-z_s)}-\frac{\frac{5}{6}(1-z_s)^2 m_w^*}{9z_f+6(z_s-z_f)+2(1-z_s)}\right) \\
& -\sum_{j=1}^{no}\left[m_c^j\left(z_s-z_f+\left(\frac{z_s-z_f}{1-h_s}h_s+z_s-z_c^j\right)\ln(h_s)\right)\right] \\
& \left.-\sum_{i=1}^{nm}\left[m_c^i\left(z_c^i-z_f+\left(\frac{z_s-z_f}{1-h_s}h_s+z_s-z_c^i\right)\ln\left(\frac{z_s-z_c^i}{z_s-z_f}(1-h_s)+h_s\right)\right)\right]\right\}; \\
K_{M_i} = {} & z_f\left\{z_s-z_f-\frac{z_s^2-z_f^2-\frac{1}{3}(1-z_s)^2(1+2\lambda_t)}{z_s(1-\lambda_t)+\lambda_t+1}\right. \\
& -\frac{\frac{1}{3}(z_s-z_f)^2(1+2\psi_s)+(1-z_s)(\psi_s+\psi_t)(z_s-z_f)+(1-z_s)^2\left(\frac{1}{3}\psi_s+\frac{2}{3}\psi_t\right)}{(1+\psi_s)(z_s-z_f)+(\psi_s+\psi_t)(1-z_s)}m_{fu} \\
& \left.-\frac{\frac{5}{2}(z_s-z_f)^2+2(1-z_s)(z_s+z_f)+\frac{5}{6}(1-z_s)^2}{9z_f+6(z_s-z_f)+2(1-z_s)}m_w^*-\sum_{i=1}^{nm}(z_c^i-z_f)m_c^i-\sum_{j=1}^{no}(z_c^j-z_f)m_c^j\right\}
\end{aligned}
\qquad (7)
$$

Table 1 Bounds on manufacturing coefficient

k_1	Stepped thickness (rather than tapered)	0.1 . . 0.13
k_2	Dead joint mass penalty	0.15 . . 0.3
k_3	Standard thickness of webs, ribs, and other elements	0.1 . . 0.13
k_4	Joint fittings and joint defects	0.1 . . 0.15
k_5	Plus toleerances	0.04 . . 0.09
k_6	Manufacturing thicknesses	0.03 . . 0.05
k_7	Breakdown joint mass penalty	0.1 . . 0.2
	$k_{man} = 1 + k_1 + k_2 + k_3 + k_4 + k_5 + k_6 + k_7$	1.62 . . 2.05

Table 2 Sample calculations for current transports

Aircraft	μ, kg	m_s, actual	m_s, formula	Error, %
B-727-100	72,600	0.111	0.1109	− 0.02
B-747-100	322,000	0.122	0.1248	2.3
DC-9-30	49,000	0.106	0.0946	−10.8
DC-10-10	195,000	0.114	0.1048	−8.1
Dc-10-30	252,000	0.106	0.1109	4.6
A-300-B2	137,700	0.145	0.1337	− 7.8
C-5A	349,000	0.13	0.1344	3.4
C-130E	68,700	0.0772	0.0759	−1.7
Tu-154	90,000	0.102	0.1066	4.6
An-10	54,000	0.0981	0.1028	4.8
An-22	250,000	0.119	0.1226	9.5
An-24	21,000	0.1142	0.1196	4.7
Il-76T	171,000	0.121	0.1237	2.2

where Λ_m is the half-chord sweep of midboard wing; Λ_o is the half-chord sweep of outboard wing; m_w^* is the previously iterated or expert-estimated relative wing structure mass; m_{fu} is the relative fuel mass; $h_s = t_s\lambda_s/t_r$ is the thickness taper to sweep joint; $h_t = t_t\lambda_t/t_r$ is the thickness taper to wing tip; $\psi_s = h_s\lambda_s$ is the wing airfoil area taper to the sweep joint; t_s is the sweep joint relative thickness; t_t is the wing tip relative thickness; and $\psi_t = h_t\lambda_t$ is the wing airfoil area taper to wing tip. The formula cannot be used for a nontapered wing because division by zero will occur if $h_s = 1$ and $h_s = h_t$. If the wing has no sweep joint, it is suggested that

$$z_s = \frac{1}{2}; \quad \Lambda_m = \Lambda_o; \quad \lambda_s = 1 - \frac{1 - \lambda_t}{2 - 2z_f};$$
$$h_s = 1 - \frac{1 - h_t}{2 - 2z_f}; \quad \psi_s = 1 - \frac{1 - \psi_t}{2 - 2z_f} \tag{8}$$

Neither simplifications nor data for mass of existing wings have been applied, so the formula completely corresponds to the concept model.[5]

Applications

The newly derived formula has been used to study the transport aircraft in Table 2. The detailed spreadsheet calculations are presented in Ref. 5. Values of the actual stresses were estimated on the basis of engineering judgment. The accuracy of the formula is within [−10.8, +9.5]% and the root-mean-square error is 5.9%. This is sufficient for most preliminary design purposes. The formula can also be improved by using statistical data.

For comparison, a previously derived formula for twin fuselage aircraft[4] can be applied to a conventional aircraft. The results yield accuracy of [−13.1, +11.7]% with root-mean-square error of 7.0%. This is not as accurate as the present formula.

References

[1]Sheinin, V. M., and Kozlowsky, V. I., *Weight Design and Effectivity of Passenger Aircraft*, 2nd ed., Mashinostroenie, Moscow, 1984 (in Russian).

[2]Eger, S. M., Mishin, W. F., Liseitsev, N. K., et al. *Aircraft Design*, Mashinostroenie, Moscow, 1983 (in Russian).

[3]Udin, S. V., and Anderson, W. J., "A Method of Wing Mass Formula Derivation," Univ. of Michigan, Aerospace Engineering Rept. SM 90.1, Nov. 1990.

[4]Udin, S. V., and Anderson, W. J., "The Complete Derivation of Wing Mass Formula for Twin Fuselage Aircraft," Univ. of Michigan, Aerospace Engineering Rept. SM 90.2, Nov. 1990.

[5]Udin, S. V., and Anderson, W. J., "The Complete Derivation of Wing Mass Formula for Subsonic Aircraft," Univ. of Michigan, Aerospace Engineering Rept. SM 91.1, April 1991.

Whirl-Flutter Stability of a Pusher Configuration in Nonuniform Flow

F. Nitzsche* and E. A. Rodrigues†
EMBRAER—Empresa Brasileira de Aeronáutica, S.A., São José dos Campos, 12225, Brazil

Introduction

IN the new aircraft configurations with pusher power plants located at the rear fuselage, the whirl-flutter stability characteristics of the engine-propeller installation may be affected by the nonuniform freeflow induced by the aircraft components positioned upstream in the flowfield. Assuming that the flowfield may still be considered stationary, the effect of the aforementioned interference is investigated. Under this assumpton, the propeller aerodynamics may be adjusted to become a periodic function of time and the aeroelastic system stability may be studied using any theory developed to analyze periodic systems. In the present work, Floquet-Liapunov's theorem[1] could be applied efficiently to evaluate the stability characteristics of an actual configuration with many interference elements.

Basic Formulation

The equation of motion of the aeroelastic system is cast in the state vector form

$$\dot{y} = A(t)y \tag{1}$$

where $A(t)$ is the matrix of influence coefficients containing the information about both the dynamics and the aerodynamics of the system. For a given set of initial conditions, the solution of this system of ordinary differential equations may be written as

$$y(t) = \Phi(t, t_0)y(t_0) \tag{2}$$

where $\Phi(t, t_0)$ is recognized to be the transition matrix relating the state vector y at the instant t to its initial value at t_0. Floquet's theorem states that in order to completely evaluate the stability characteristics of a periodic system, it will suffice

Presented as Paper 90-1162 at the AIAA/ASME/ASCE/AHS/ASC 31st Structures, Structural Dynamics and Materials Conference, Long Beach, CA, April 2–4, 1990; received Nov. 23, 1990; revision received Sept. 2, 1991; accepted for publication Sept. 26, 1991.

*Senior Engineer, Aeronautical Engineering Division; currently Postdoctoral Fellow, DLR/Institut fuer Aeroelastik, Bunsenstrasse 10, W-3400 Goettingen, Germany. Member AIAA.

†Staff Engineer, Aeronautical Engineering Division; currently Graduate Student, Purdue Univ., School of Aeronautics and Astronautics, West Lafayette, IN 47907.